

Nanostructured magnetic alginate composites for biomedical applications

Pedro Marins Bedê¹, Marcelo Henrique Prado da Silva^{1*}, André Bem-Hur da Silva Figueiredo¹ and Priscilla Vanessa Finotelli²

¹Instituto Militar de Engenharia – IME, Rio de Janeiro, RJ, Brazil

²Faculdade de Farmácia, Centro de Ciências da Saúde – CCS, Universidade Federal do Rio de Janeiro – UFRJ, Rio de Janeiro, RJ, Brazil

*marceloprado@ime.eb.br

Abstract

This is a study of the preparation and characterization of polymeric-magnetic nanoparticles. The nanoparticles used were magnetite (Fe_3O_4) and the chosen polymers were alginate and chitosan. Two types of samples were prepared: uncoated magnetic nanoparticles and magnetic nanoparticles encapsulated in polymeric matrix. The samples were analyzed by XRD, light scattering techniques, TEM, and magnetic SQUID. The XRD patterns identified magnetite (Fe_3O_4) as the only crystalline phase. TEM analyses showed particle sizes between 10 and 20nm for magnetite, and 15 and 30nm for the encapsulated magnetite. The values of magnetization ranged from 75 to 100emu/g for magnetite nanoparticles, and 8 to 12emu/g for coated with chitosan, at different temperatures of 20K and 300K. The saturation of both samples was in the range of 49 to 50KOe. Variations of results between the two kinds of samples were attributed to the encapsulation of magnetic nanoparticles by the polymers.

Keywords: *alginate, chitosan, composite, nanoparticles, magnetic.*

1. Introduction

Major advances in science have allowed the nanotechnology emerge as one of the most promising research areas, in especially for their potential biomedical applications. This paper focuses on developing a route for the production of magnetic nanoparticles encapsulated in a polymeric matrix, providing the basis from which the applied research can be established. Among the biomedical applications of magnetic nanoparticles, controlled drugs delivery and hyperthermia in cancer treatment are possible trends. Controlled drug delivery systems can be defined as those in which the active agent is released regardless of external factors and have well-established kinetics. These delivery systems offer several advantages when compared to other conventional systems, such as increased therapeutic efficacy, along with progressive and controlled drug release from the matrix degradation or externally controlled by diffusion, significant reduction of the toxicity and increasing remaining time in the bloody system, varied nature and composition of the vehicles and, contrary from what it might be expected, there is no predominance of instability and decomposition mechanisms of the drug (premature bio-inactivation), safe and convenient administration, with few doses and without local inflammatory reactions, directing to specific targets without significant immobilization of bioactive species, both substances hydrophilic and lipophilic can be incorporated^[1]. Hyperthermia is a promising therapy for cancer treatment. The components involved in this therapy are magnetic materials such as iron oxides (ferrofluids) and techniques applying an oscillating magnetic field. The application of this field in magnetic fluids are able to generate heat by converting magnetic energy into heat, raising the local temperature up to 41-46°C. This temperature range can

kill tumor cells without killing normal cells^[2]. According to Zhao et al.^[2], the magnetic particles convert the energy of the oscillating magnetic field into heat by physical mechanisms and the efficiency of this conversion is strongly dependent on the external field frequency and on the particles nature. This heating is dependent on the size and microstructure of the particles, as these characteristics will deeply influence their magnetic properties^[3]. The tumor cells are sensitive to temperature variations. Thus, in the presence of ferrofluids and applied magnetic field, the magnetic nanoparticles can eliminate tumor cells in vivo and in vitro by hyperthermia^[4]. This application requires that the magnetic nanoparticles show high magnetization values for high values of thermal energy, being these particles smaller than 50 nm, with a narrow particle size distribution. Furthermore, for application in hyperthermia, these magnetic nanoparticles require special surface coating, that should be not only non-toxic and biocompatible, but also allow the targeting of particles to a specific area. Because of their hydrophobic surfaces and large surface area relative to volume, the magnetic nanoparticles tend to agglomerate and be released quickly by movement. It is possible to avoid this effect by coating the nanoparticles with biocompatible polymers^[5].

Among magnetic nanoparticles, the ones that have attracted attention in biomedical applications are iron oxide nanoparticles, more precisely magnetite (Fe_3O_4) and maghemite ($\gamma\text{-Fe}_2\text{O}_3$). Magnetite ores are the most used source for obtaining iron. This ore is a mix of iron oxides, with FeO and Fe_2O_3 having spinel structure of inverted O^{2-} ions with cubic packing, the larger Fe^{2+} ions in the octahedral interstices, half of Fe^{3+} ions in octahedral sites and half of

the remaining in tetrahedral positions. The magnetization of Fe_3O_4 occurs in the presence of external magnetic field, and disappears when the field is removed. This effect is due to non-conservation of magnetic orientation of individual atoms^[6]. As for the polymeric matrix, the alginate is a very consistent choice, because it is biocompatible, allows its use in biomedical applications. It also forms a strong gel in the presence of divalent cations, especially calcium, by ionic crosslinks between the polyionic alginate chains^[7]. This gelation of alginate is conventionally described in terms of the “egg box” model, where divalent cations are coordinately bound to the carboxyl groups of guluronic acid^[8]. This model is shown in Figure 1. The structure of guluronic acid provides the right distance between the carboxyl and hydroxyl groups, with a high coordination degree with calcium Ca^{2+} cations^[10].

2. Materials and Methods

The materials used in all stages of polymer-magnetic nanoparticles were purchased from Fluka – Biochemika (sodium alginate), Aldrich (chitosan), and VETEC (calcium chloride and ammonium hydroxide).

Magnetite was obtained by the co-precipitation method from Fe II and Fe III in an alkaline medium according to the reaction:

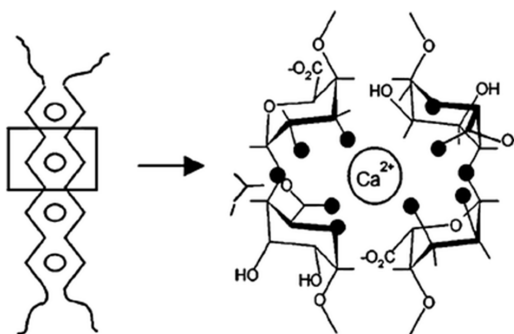
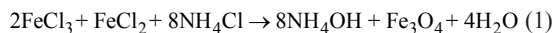


Figure 1. “Egg-box” model for Calcium Alginate^[9].

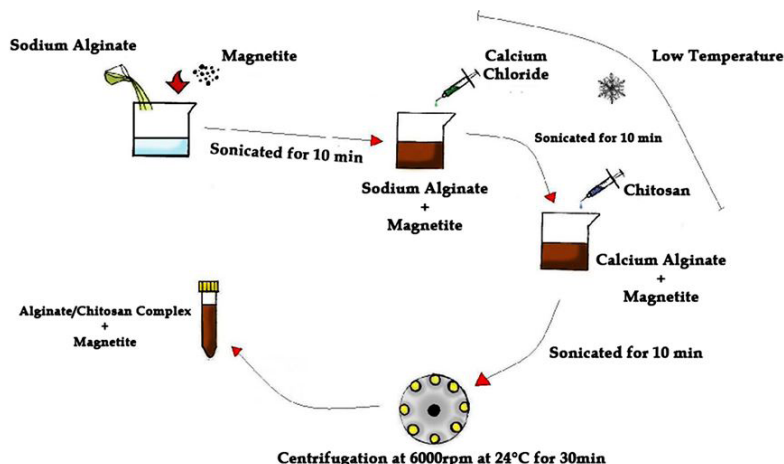


Figure 2. Schematic illustration of the magnetite encapsulation process.

FeCl_2 and FeCl_3 solutions were mixed and kept under mechanical stirring at 60°C during 15 minutes. The next step was to drop 200 mL of 25% ammonium hydroxide (NH_4OH) were drop into the $\text{FeCl}_2 + \text{FeCl}_3$ mixture. The precipitate was washed with 50 ml of distilled water, centrifuged and lyophilized.

2.1 Encapsulation of Fe_3O_4 in the alginate/chitosan matrix

The first step was to prepare three different solutions:

- Sodium alginate – 9.5 ml, 0.06%;
- Calcium chloride – 0.5 ml, 18 mM;
- Chitosan – 2 ml, 0.05%.

Sodium alginate solution was mixed with 0.0024 g of magnetite.

The alginate + Fe_3O_4 solution was constantly sonicated (probe sonicator), so that complete mixing of the solutions could occur. CaCl_2 solution was slowly dripped and sonicated. After complete mixing, chitosan was added to the calcium alginate and magnetite mixture, and then sonicated, remaining under stirring during further 20 min and centrifuged at 6000 rpm at 24°C during 30 min. The scheme of this process can be seen in Figure 2.

In order to characterize nanoparticles, the following techniques were applied:

X-Ray Diffraction was performed on X’Pert PRO (Panalytical) equipment. The method used was the powder method, using copper $\text{K}\alpha 1$ radiation with wavelength (λ) 1.54056 Å. The measurements were performed with 40 mA and 40 kV.

Size and Zeta Potential was performed on a ZETA PLUS ANALYZER equipment, from BROOKHAVEN INSTRUMENTS CORPORATION company. The ZETA PLUS parameters used were: five runs of 30 seconds each in ultrapure water with refractive index 1.340.

Transmission Electron Microscopy was performed on a FEI Tecnai G20 equipment, with 200 kV voltage.

Magnetic Measurements (SQUID) was performed using Quantum Design MPMS-5S SQUID magnetometer.

3. Results and Discussion

3.1 X-Ray Diffraction (XRD)

X-Ray diffraction analyses were performed for Fe_3O_4 and Fe_3O_4 encapsulated in alginate/chitosan complex polymer. Figure 3 shows the diffraction pattern characteristic of magnetite (JCPDS 19-0629). Figure 4 presents the diffraction pattern obtained for the encapsulated magnetite, where the presence of amorphous material is evident. The amorphous phase was associated to the complex alginate with chitosan. The good definition of the reflection peaks in the Fe_3O_4 sample, resulting in a well-defined diffraction pattern, confirms the success of the synthesis method for the production of well crystallized magnetite as fabricated. The crystallite size was 10 nm, determined by Scherrer's method.

3.2 Size and zeta potential

The size measurements are important to define the best method of sample preparation, since it enables the choice for a size range that will provide the desired material properties. The mean diameter of magnetic nanoparticles, as shown in Table 1, was 155.8 nm with a polydispersity average of 0.213. The diameter for the the magnetic nanoparticles encapsulated, shown in Table 2, was 254.9 nm with a polydispersity average of 0.329. These tables show a polydispersity narrow size distribution and homogeneity of the nanoparticle, indicating stability and control of the

diameter^[11]. In a previous study, Ma et al.^[12] synthesized nanoparticles of magnetite (Fe_3O_4) coated with alginate, and found an average diameter of 193.8 nm and polydispersity index of 0.209. Ahmad et al.^[13] synthesized nanoparticles of alginate/chitosan and obtained with an average diameter of 229 nm polydispersity of 0.44 of these nanoparticles. It is important to emphasize that this is probably related to the diameter of agglomerates and not the isolated nanoparticles. A possible confirmation that may arise through the analysis of transmission electron microscopy is the fact that the encapsulated nanoparticles showed higher average size than non-encapsulated may be associated with the own polymer coating these nanoparticles. Due to these small sizes, the material is expected to present the desired magnetic properties, but this can only be confirmed through the characterization of these properties.

The zeta potential measurements were performed in order to find out if the material exhibited good stability when in suspension. The general rule for electrostatic stability of the solution is the Zeta potential range of +/- 30 mV. As the zeta potential of the three samples is outside this range, we can consider that the samples are stable. An important factor to be considered is the presence of chitosan in the material. One can perceive a potential variation between samples with and without chitosan, the ones with chitosan being more stable. This can be a direct consequence of the fact that chitosan acts as an inhibitor of surface charges existing in the alginate, thereby contributing to a better stability. Table 3 shows the change in nanoparticle Zeta potential between the coated and non-coated samples.

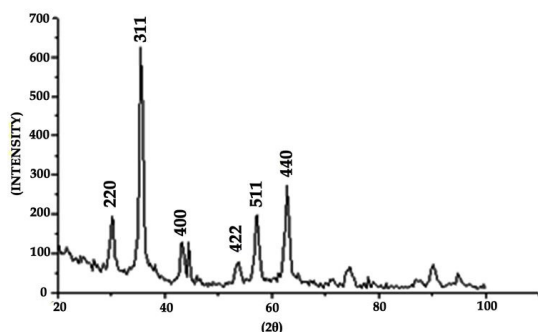


Figure 3. XRD pattern of magnetic nanoparticles.

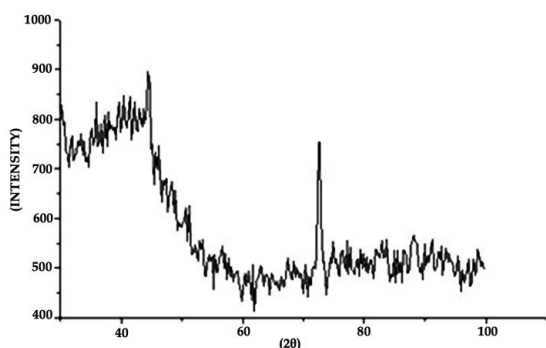


Figure 4. XRD pattern of magnetic nanoparticles encapsulated in polymeric matrix.

Table 1. Size of magnetic NP.

MEASUREMENTS	DIAMETER (nm)	POLYDISPERSITY
1	150.4	0.195
2	160.9	0.242
3	145.1	0.190
4	163.4	0.209
5	159.2	0.231
AVERAGE	155.8	0.213
ERROR	3.5	0.010

Table 2. Size of magnetic NP encapsulated in polymeric matrix.

MEASUREMENTS	DIAMETER (nm)	POLYDISPERSITY
1	230.0	0.677
2	248.7	0.199
3	260.6	0.327
4	271.9	0.260
5	263.7	0.184
AVERAGE	254.9	0.329
ERROR	7.3	0.091

Table 3. Zeta potential of the nanoparticles.

pH	Sample	Average Zeta Potential
3.61	PM-NP w/ chitosan	$-(37.59 \pm 2.9)$ mV
3.61	PM-NP	$-(30.63 \pm 0.8)$ mV
3.61	Magnetic NP	$-(30.45 \pm 2.7)$ mV

3.3 Transmission Electron Microscopy (TEM)

Figure 5 refers to magnetic nanoparticles without encapsulation. A nearly spherical shape and a strong trend to agglomerate can be observed. The particles diameter is between 10 and 20 nm, which allows these nanoparticles to present superparamagnetic behavior. In a previous work, Kim et al.^[5] synthesized Fe_3O_4 nanoparticles coated with chitosan and observed average diameter of 10.3 nm.

Figure 6 refers the magnetic nanoparticles encapsulated in polymeric matrix (PM-NP). It can be observed that the coated particles were more dispersed, when compared

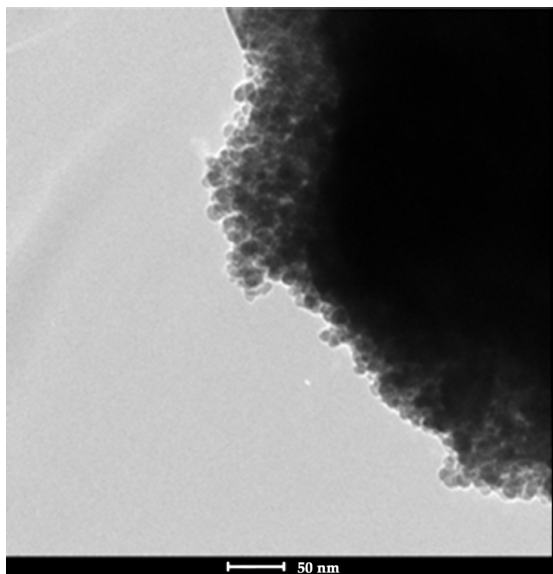


Figure 5. Electromicrograph (TEM) of uncoated magnetic nanoparticles.

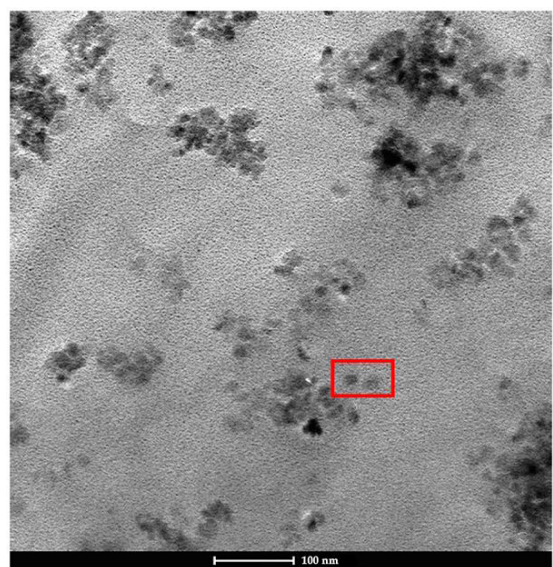


Figure 6. Electromicrograph (TEM) of magnetic nanoparticles encapsulated in polymeric matrix (PM-NP). The rectangle shows the area from which EDS was performed.

to uncoated ones. This finding may be linked to the fact that magnetic nanoparticles are encapsulated in a matrix of alginate and chitosan; chitosan, acting as an inhibitor of surface charges, has resulted in a better stability of the nanoparticles. Regarding the size, the observed diameter was in the range of 15 to 30nm, which allows these PN-PM to present superparamagnetic behaviors. TEM analyses also confirmed that the diameter size found in the analysis by light scattering techniques is related to the clusters of nanoparticles. In a previous study, Ma et al.^[12] observed average diameter of 10nm in NP-PM magnetite (Fe_3O_4) coated with alginate. Energy dispersive spectroscopy (EDS) was also carried out for the PM-NP nanoparticles, highlighted by the red rectangle region in Figure 6. The presence of the elements Ca, Fe and C was confirmed.

3.4 Magnetic measurements (SQUID)

The magnetization measurements of samples A and B were performed at temperatures 20 K and 300 K. Figure 7 refers to uncoated samples, while Figure 8 refers to coated samples. At 20 K, the saturation field of the samples A and B was approximately 50 KOe, and 300 K of 49 KOe. The results for the maximum magnetization of the Fe_3O_4 nanoparticles

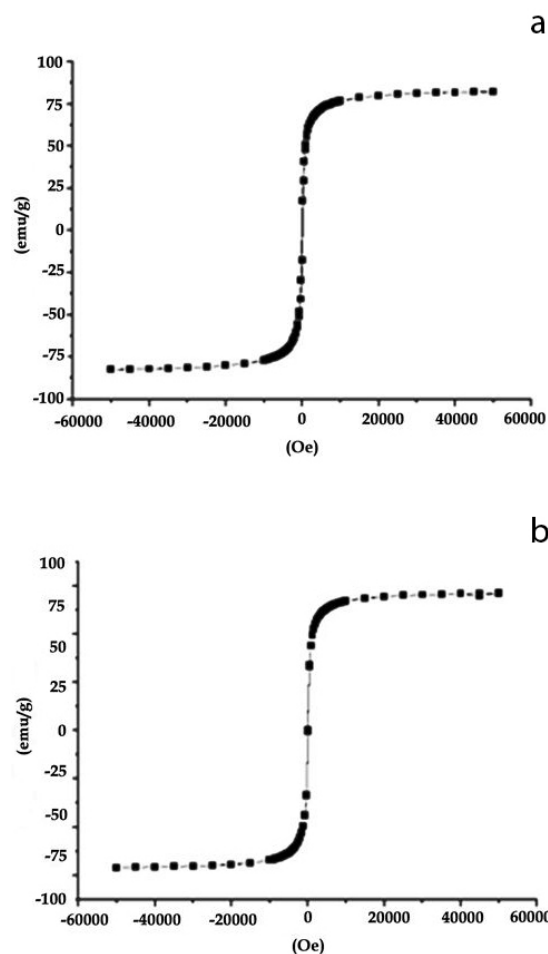


Figure 7. MxH curve at 20K (a) and 300K (b) of magnetite nanoparticles.

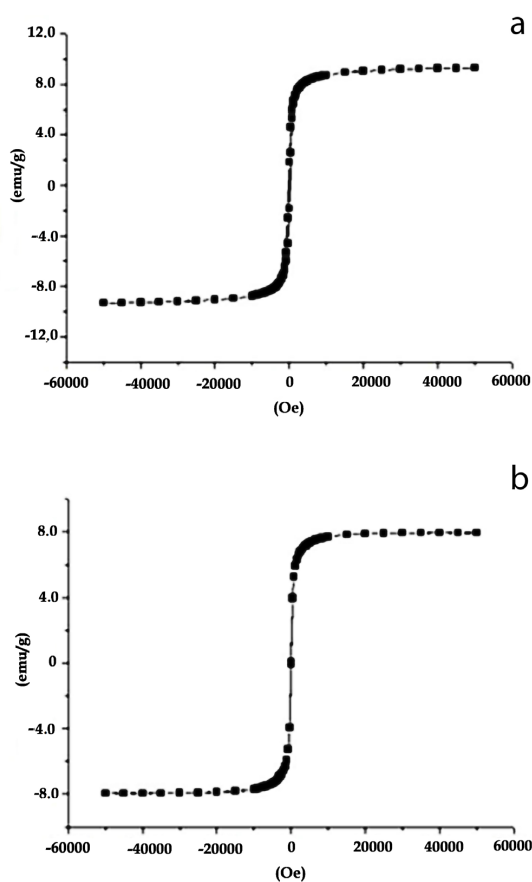


Figure 8. MxH curve at 20K (a) and 300K (b) of encapsulated magnetite nanoparticles.

without coating ranged from 75 to 100 emu/g at 300 K and 20 K, respectively, and Fe_3O_4 nanoparticles in the coating ranged from 8 to 12 emu/g at 300 K and 20 K, respectively. A decrease in the magnetization was observed at 300 K for both samples. A further reduction was also observed, when comparing coated and uncoated samples. This reduction may be explained by the encapsulation, being the polymers a barrier to magnetization. If the alginate completely covers Fe_3O_4 nanoparticles, the magnetization will drop significantly^[14]. This reduction can also be associated with two factors: the drying of the encapsulated samples, and especially the concentration of Fe_3O_4 used in their preparation. Another important fact to note is that both samples at 20 K and 300 K, showed virtually no hysteresis, presenting coersivity almost nil. This may confirm the superparamagnetic character of the samples. In a previous study, Ma et al.^[12] found values for the magnetization of magnetite nanoparticles (Fe_3O_4) encapsulated in alginate matrix ranging from 30 to 55 emu/g at room temperature. Ma et al.^[12] associated with this variation to the concentration of Fe_3O_4 used in the synthesis of their samples; the saturation field found by Ma et al.^[12] in all samples was slightly higher than 10 KOe, a value almost six times smaller when compared to those found in the present study.

4. Conclusions

With the intention to produce encapsulated magnetic particles for possible use biomedical applications, alginate and magnetite nanoparticles were successfully synthesized. The nature of the iron oxide (magnetite, Fe_3O_4) was confirmed by identification of diffraction peaks in XRD analysis. Crystallite size was determined by the Debye-Scherrer method and found an average diameter of 10nm. The material presented good stability, measured by the zeta potential and ideal size, which could be measured by light scattering and transmission electron microscopy. Microscopy also allowed to provide a morphological analysis of the material, confirming the expected nearly spherical shape of the nanoparticles. The good magnetization and superparamagnetic character of the material was confirmed by the measurements of the magnetic SQUID.

5. Acknowledgements

The authors would like to acknowledge to CNPq, CAPES, CEPTEL and CBPF.

6. References

1. Kumar, R. (2000). Nano and microparticles as controlled drug delivery devices. *Journal of Pharmacy & Pharmaceutical Sciences*, 3(2), 234-258. PMID:10994037.
2. Zhao, D., Zeng, X., Xia, Q., & Tang, J. (2006). Inductive heat property of Fe_3O_4 nanoparticles in AC magnetic field for local hyperthermia. *Rare Metals*, 25(6), 621-625. [http://dx.doi.org/10.1016/S1001-0521\(07\)60159-4](http://dx.doi.org/10.1016/S1001-0521(07)60159-4).
3. Atsumi, T., Jeyadevanb, B., Satob, Y., & Tohji, K. (2007). Heating efficiency of magnetite particles exposed to AC magnetic field. *Journal of Magnetism and Magnetic Materials*, 310(2), 2841-2843. <http://dx.doi.org/10.1016/j.jmmm.2006.11.063>.
4. Jordan, A., Scholz, R., Wust, P., Fähling, H., & Roland Felix (1999). Magnetic fluid hyperthermia: cancer treatment with AC magnetic field induced excitation of biocompatible superparamagnetic nanoparticles. *Journal of Magnetism and Magnetic Materials*, 201(1-3), 413-419. [http://dx.doi.org/10.1016/S0304-8853\(99\)00088-8](http://dx.doi.org/10.1016/S0304-8853(99)00088-8).
5. Kim, D. H., Lee, S. H., Im, K. H., Kim, K. N., Kim, K. M., Shim, I. B., Lee, M. H., & Lee, Y.-K. (2006). Surface-modified magnetite nanoparticles for hyperthermia: preparation, characterization, and cytotoxicity studies. *Current Applied Physics*, 6(S1), 242-246. <http://dx.doi.org/10.1016/j.cap.2006.01.048>.
6. Sidhu, P. S., Gilkes, R. J., & Posner, A. M. (1978). The synthesis and some properties of Co, Ni, Zn, Cu, Mn and Cd substituted magnetites. *Journal of Inorganic and Nuclear Chemistry*, 40(3), 429-435. [http://dx.doi.org/10.1016/0022-1902\(78\)80418-7](http://dx.doi.org/10.1016/0022-1902(78)80418-7).
7. Boissesson, M. R., Leonard, M., Hubert, P., Marchal, P., Stequeart, A., Castel, C., Favre, E., & Dellacherie, E. (2004). Physical alginate hydrogels based on hydrophobic or dual hydrophobic/ionic interactions: Bead formation, structure, and stability. *Journal of Colloid and Interface Science*, 273(1), 131-139. PMID:15051442. <http://dx.doi.org/10.1016/j.jcis.2003.12.064>.
8. Iskakov, R. M., Kikuchi, A., & Okano, T. (2002). Time-programmed pulsatile release of dextran from calcium-alginate gel beads coated with carboxy-n-propylacrylamide copolymers. *Journal of Controlled Release*, 80(1-3), 57-68. PMID:11943387. [http://dx.doi.org/10.1016/S0168-3659\(01\)00551-X](http://dx.doi.org/10.1016/S0168-3659(01)00551-X).
9. Shao, F., Ankur, T., Diana, M. S., Riccardo, L. B., Ira, S. B., Sachin, V., Eric, J. M., & Lawrence, H. B. (2011). Relevance

- of rheological properties of sodium alginate in solution to calcium alginate gel properties. *AAPS PharmSciTech*, 12(2), 453-460. PMID:21437788. <http://dx.doi.org/10.1208/s12249-011-9587-0>.
10. Finotelli, P. V. (2006). *Microcápsulas de alginato contendo nanopartículas magnéticas para liberação controlada de insulina* (Tese de doutorado). Instituto de Química, Universidade Federal do Rio de Janeiro, Rio de Janeiro.
 11. Kulkamp, I. C., Paese, K., Guterres, S. S., & Pohlmann, A. R. (2009). Estabilização do ácido lipoico via encapsulação em nanocápsulas poliméricas planejadas para aplicação cutânea. *Química Nova*, 32(8), 2078-2084. <http://dx.doi.org/10.1590/S0100-40422009000800018>.
 12. Ma, H., Qi, X. R., Maitani, Y., & Nagai, T. (2007). Preparation and characterization of superparamagnetic iron oxide nanoparticles stabilized by alginate. *International Journal of Pharmaceutics*, 333(1-2), 177-186. PMID:17074454. <http://dx.doi.org/10.1016/j.ijpharm.2006.10.006>.
 13. Ahmad, Z., Pandey, R., Sharma, S., & Khuller, G. K. (2006). Pharmacokinetic and pharmacodynamic behaviour of antitubercular drugs encapsulated in alginate nanoparticles at two doses. *International Journal of Antimicrobial Agents*, 27(5), 409-416. PMID:16624533. <http://dx.doi.org/10.1016/j.ijantimicag.2005.12.009>.
 14. Denizot, B., Tanguy, G., Hindre, F., Rump, E., & Jeune, J. J. L. & Jallet, P. (1999). Phosphorylcholine coating of iron oxide nanoparticles. *Journal of Colloid and Interface Science*, 209(1), 66-71. PMID:9878137. <http://dx.doi.org/10.1006/jcis.1998.5850>.

Received: Aug. 11, 2015

Revised: Mar. 11, 2016

Accepted: May 17, 2016